

www.acsaem.org Article

Effect of Long-Lived Ground-State Diradicaloids on the Photophysics of Semiladder Thiophene-Based Polymer Aggregates for Organic Light-Emitting Transistor Applications

Angelar K. Muthike, Mohammad Ahmad Awais, Cong Wang, Meghan E. Orr, Nuno M.S. Almeida, Sasha C. North, Luping Yu, Angela K. Wilson, and Theodore G. Goodson, III*



Cite This: ACS Appl. Energy Mater. 2024, 7, 4904–4918



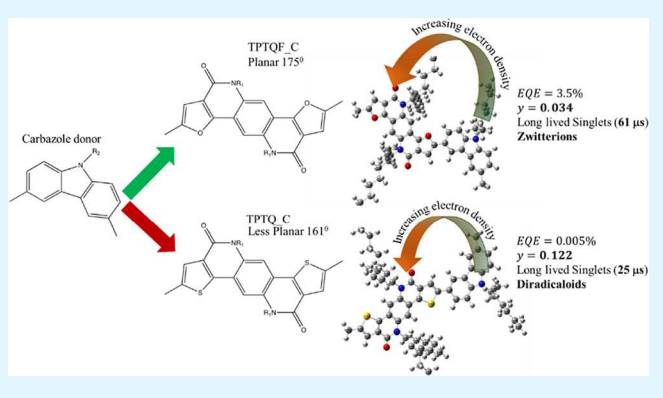
ACCESS I

III Metrics & More

Article Recommendations

s Supporting Information

ABSTRACT: To fully utilize the immense potential of organic light-emitting transistors (OLETs), the mechanism of charge transfer in these devices needs to be better understood. The majority of prior studies have leaned toward understanding either organic light-emitting diodes (OLEDs) or organic field-effect transistors. Recently, there has been an interest in the use of openshell structures, which have been reported to enhance the spin density that is delocalized along the planar π -conjugated backbone, ultimately affecting their charge transfer and the overall device performance efficiency. These structures tend to have low-lying triplets and small singlet—triplet energy gaps, which are favorable for charge and energy transfer for OLET applications. Open-shell diradicals have been reported to enhance the efficiency of OLEDs



by offering intermolecular spin—spin interactions, which lead to σ -aggregation. This σ -aggregation eventually leads to the formation of σ -polymerization, affecting intermolecular stacking and charge transport, which has been useful for OLEDs. However, it is unknown how diradical states affect the efficiency of OLETs. In this study, we utilize both linear and nonlinear spectroscopic techniques to probe the dynamics of diradical states in novel organic thiophene systems. We also utilize computational methods to probe the energies of the electronic states of the diradical systems investigated. For the furan-containing polymer system, we found the formation of long-lived zwitterions. We propose that the formed diradical character with a lifetime of 25 μ s lowers the charge transport in the resonant structures, reducing charge transfer and negatively affecting the external quantum efficiency of the thiophene-based OLETs.

KEYWORDS: organic field-effect transistors, linear and nonlinear spectroscopic, thiophene, diradical, time-resolved spectroscopy

1. INTRODUCTION

Organic light-emitting transistors (OLETs), first reported in 2003, are a promising class of organic optoelectronic devices that have the unique advantage of combining the electrical switching functionality of organic field-effect transistors (OFETs) and the light generation capability of organic lightemitting diodes (OLEDs) in a single device. 1-3 While OFET and OLED technologies are significantly developed, the working mechanisms and principles of OLETs as well as their potential have not been fully exploited.²⁻⁴ Prior research has shown that OLETs have immense potential to reduce the complexity and enhance the performance of next-generation pixel circuitry.2 OLETs have shown significant potential toward applications such as optical communications systems, electroluminescent displays, electrically pumped organic lasers, and solid-state lighting sources. 2,5 However, the applicability of these OLETs is far from implementation due to their poor

performance in terms of low brightness, low carrier mobility, and high driving voltage.⁶

A typical material for OLET applications will exhibit high charge mobility as well as increased fluorescence quantum yield in the same material. Recent reports have shown that organic semiconducting (OSC) materials for these OLET devices are made of small molecules and polymers that hold the right luminescent properties, have small bandgaps in the visible region of the electromagnetic spectra to minimize charge injection barriers, possess high, balanced and ideally ambipolar charge carrier mobility for light emission, and have

Received: March 20, 2024 Revised: May 13, 2024 Accepted: May 13, 2024 Published: May 27, 2024





Figure 1. Structures of the investigated polymers (TPTQ C and TPTQF C and their respective resonant forms) as well as the TPTQ acceptor.

high shelf life.8 The increased interest in small molecules as potential OLET active materials is due to their molecular structure and high-mobility characteristics. The delocalization of π -bonds in these small molecules and polymers leads to good photoabsorption, charge carrier photogeneration, and transport, making these materials great for OLET applications. Although conjugated polymers have shown a lot of promise as OLET materials, a major drawback in using these lightemitting polymers is their low charge carrier mobility, which limits device performance. A small bandgap for the conjugated polymers is preferable to enhance the intramolecular charge transfer across the main donor-acceptor chain, with a lowerlying lowest unoccupied molecular orbital (LUMO), which is better for n-type OLETs. 10 In addition, these donor-acceptor polymers induce intermolecular interactions through increased molecular ordering resulting from the self-assembly of polymer chains, and this effect has led to high field-effect mobility in OFETs.1

While single-component OLETs have been successfully developed, only an external quantum efficiency (EQE) of 1.61% has been reported. 12 Due to the difficulties in attaining large mobilities in single OLET materials, multilayer devices where different functions are delegated to different materials have been developed leading to improved EQEs of up to 9.01%.6 For the multilayered devices, however, the device fabrication process becomes extremely complicated as more layers are added. This is due to the fact that it becomes very difficult to control the mutually exclusive device properties of the OSC active materials while keeping their optoelectronic performance optimal.⁹ For instance, high mobility materials show efficient intermolecular charge transport owing to their optimal $\pi - \pi$ stacking and electronic coupling; the efficient π - π stacking may lead to the formation of excited state dimers or other charge transfer states, which quench fluorescence and reduces the performance of OLETs.³ Therefore, it is important

to find a balance between the multiple parameters that should be considered when fabricating high-performance OLET systems: suitable energy levels, optimal fluorescent quantum yields, optimal charge mobility, and correct aggregation state. ^{7,9,10,13}

Recently, Yuan et al.⁵ synthesized semiladder polymer systems that not only address the mobility issues but are also the first-of-a-kind OLET systems that exhibit a folding structure that has only been previously observed and wellstudied in biological systems.⁵ These biological macromolecules have shown the existence of foldamers that adopt highly ordered and helical self-assembled structures through noncovalent interactions. 5,14-16. The idea of using foldamers was that this structural twist would improve the materials' electrical and light-emitting properties.⁵ The structures of the two investigated polymers and the thiophene-based acceptor (TPTQ acceptor) are shown in Figure 1. Here, two different acceptor (A) monomers: thienopyridothienoquinoline, which has a thiophene incorporated (TPTQ C), and thienopyridothienoquinoline, with a furan molecule incorporated (TPTQF C), (each acceptor coupled to a carbazole donor (D) monomer moiety) were synthesized. These D-A-Dpolymers were synthesized based on the idea that ring fusion in the ladder building blocks can enhance rigidity in the molecular system, which minimizes the nonradiative decay and thus improves fluorescence quantum yield. Interestingly, Yuan et al. reported that these structures can exist in their electron resonant forms as a result of their quadrupole interactions forming $D-A^--D^+$ structures, which tend to display nonkasha spectroscopic behavior. 5,13,17 Furan derivatives have been reported to be better than thiophene derivatives in terms of solubility, increased power conversion efficiencies, and formation of quinoidal structures owing to the lack of aromaticity in sulfur in comparison to thiophene. While thiophene-based molecules have been highly inves-

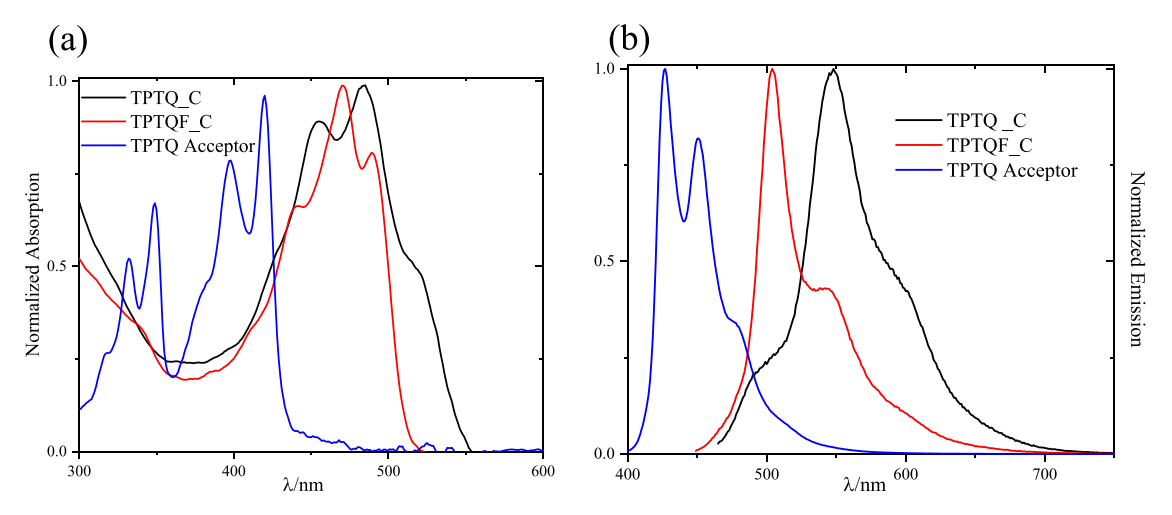


Figure 2. Absorption (a) and emission (b) spectra of the two investigated polymers as well as of the parent thiophene-based acceptor.

tigated due to their abilities to increase molecular conjugation, furan-based counterparts are seemingly promising due to their reported tendency to increase conjugation and improve charge transport properties.¹⁸ The furan-based molecules have shown enhanced performance, which has been linked to their increased dipole moments, and weak solid-state interaction between furan moieties, making them highly soluble.

Additionally, Yuan et al. reported that these polymers have the special ability to form foldable structures and exist in their resonant forms.⁵ Prior work showed that folding structures form ordered and helical self-assembled structures through noncovalent interactions. 5,14,15 The molecular conformation is rigidified by intramolecular hydrogen bonding, leading to strong interactions between the layers. 19 These π -conjugated compounds are believed to form helical conformations through solvophobic interactions in polar solvents and unravel into a random coil in chloroform. 20 Moreover, quinoline structures are able to exist in their electron resonant forms while carbazole-based molecules can form zwitterions and diradicals, which then affect the energy and charge transfer mechanisms of their derivatives.^{21–24} Interestingly, some singlet diradical states have been reported to transition to singlet zwitterion states where the latter is at higher energy.^{25–2}

It appears that many prior studies have used the terms diradicals and biradicals interchangeably, which leads to confusing and conflicting information regarding their respective photophysical properties and their effect on device performance. While both are defined by the presence of two unpaired nonbonding and degenerate electrons (radicals) in an open-shell structure, the distance between the two unpaired electrons (r) as well as the electron exchange integral (J) can be used to differentiate between these two states. For biradicals, the distance between the two nonbonding electrons is so long that the electron exchange interaction is negligible. It is defined as an even-electron molecular structure with two free radical centers, which act independently of each other. On the other hand, when the coupling between the two nonbonding electrons is strong, due to a large magnitude of dipole-dipole interaction in a molecule, one finds an example of the general class of diradicals. The molecular structures are even-electron molecules but have one fewer bond than the number permitted by the octet rule.²⁸ For nearly degenerate molecular orbitals, the terms used are diradicaloids or biradicaloids for diradicals and biradicals, respectively.

Recently, organic semiconductors showing open-shell diradical character that could be used in organic electronic materials such as OLEDs, organic photovoltaics (OPVs), and OFETs have been reported.^{24,29-33} Increased diradical character has been reported to activate exothermic singlet exciton fission, which increases the performance and stability of OPVs.³⁴ Diradical character has also been reported to affect the optical, electronic, magnetic properties, and the chemical reactivity of organic optoelectronic materials.³⁵ This is due to the presence of unpaired electrons that take part in the low- to high-spin state transitions. In addition, prior studies have shown the diradical effect on OFETs, increasing the stability and half-life of these optoelectronics. 36-38 In a recent review, Dong and Li suggested that the ground states of these materials are highly controversial due to their high reactivity toward oxygen. To mitigate stability issues, they suggested using substituents like mesityl on S atom acene analogues and bulky compounds which led to half-lives of more than a month.³⁸ Delocalization of these radials on the organic π system dilates the spin density of the molecules and therefore reduces their reactivity. In another report, neutral radicals from various open-shell molecules have been used to fabricate OLEDs with up to 10% EQE. 32,39 Because luminescent radicals emit from the radiative decay of doublet excitons, the theoretical internal quantum efficiency can be up to 100%. However, although much research has been done in synthesizing these materials, very little is known about the photophysics and charge transfer mechanisms that affect their EQEs. To the best of our knowledge, no one has reported the existence of diradical character in OLET foldamers, which would highly affect their energy transfer process and efficiency.

In this study, time-resolved and nonlinear spectroscopic techniques are used to show the formation and effect of triplet ground state diradicals on the photophysical properties of synthesized carbazole-donor-based foldable polymers for OLET applications. Thiophene-acceptor-based foldamers show a diradical character with reduced dipole moments, which lowers the charge separation in the resonance structures, reducing the charge transfer and the EQE of the TPTQ_C molecule (0.005%). However, there is no observed diradical character in the furan-based foldamers, exhibiting superior device performance with 3.5% EQE. Our results provide a step forward toward producing materials that can be used for high-performance devices.

Table 1. Linear Optical Properties for the Investigated Polymers (TPTQ_C and TPTQF_C) and the TPTQ Acceptor in Chloroform

compound	λ_{abs} (nm)	$\lambda_{\rm em}$ (nm)	$egin{pmatrix} \lambda_{ m Phosph.} \ (m nm) \end{pmatrix}$	Stokes shift (cm ⁻¹)	$\varepsilon (\mathrm{M^{-1} cm^{-1}})$	$\phi_{ ext{ iny F}}\%$ (UP)	$\phi_{\scriptscriptstyle m F}\%$ (P)	δ TPA/GM $\lambda_{\rm exc}$ = 790 nm
TPTQ acceptor	332, 348, 397, <u>419</u>	<u>426</u> , 450, 477	844	392	4261	14	11	67.4
TPTQ_C	455, <u>483</u> , 520	492, <u>548</u> , 600	970	2456	42437	38	36	223
TPTQF_C	440, <u>470</u> , 489	<u>504</u> , 544	944	1435	42505	44	42	289

2. RESULTS

2.1. Steady-State Measurements Studies. The steady-state absorption and emission spectra for the investigated polymers and those of the TPTQ acceptor are shown in Figure 2. These measurements were done in chloroform, and the data is summarized in Table 1. In Figure 2a, both of the polymers show two distinct absorption bands that have been reported for donor—acceptor polymers. The two absorption bands for the TPTQ acceptor may suggest some level of charge transfer occurring within the acceptor itself. In addition, the full-width half max (fwhm) of the polymer absorption spectrum (right absorption band) is significantly larger than that of the TPTQ acceptor. This larger fwhm suggests that the polymers may have a better capability to harvest sunlight at longer spectral regions. 40

For the polymers, the broader absorption maxima peaks, which are red-shifted, can be attributed to the highest occupied molecular orbital (HOMO) \rightarrow LUMO transition, which signifies intramolecular charge transfer between the donor and the acceptor. The slightly red-shifted absorption spectra of the TPTQ_C indicate that this polymer has a lower HOMO–LUMO bandgap and is expected to show enhanced charge transfer capabilities compared to its furan-based TPTQF_C analogue. Interestingly, a weak low-energy shoulder is very visible in the broadened absorption of the TPTQ_C molecule at 520 nm. The absorption bands in the blue have been attributed to localized π - π * transitions. The steady-state absorption for TPTQF_C is narrower, and its maximum peak is blue-shifted in comparison to that of TPTQ_C.

The decrease in the absorption intensity ratio in a comparison of the absorption spectra of the TPTQ acceptor to those of the polymer molecules suggests that these polymers form H-aggregates. These H-aggregates exist even at the level of a single polymer chain as shown by the consistent spectral appearance at very low concentrations (Figure 2). This may suggest that the polymer is folded to enhance H-aggregation, leading to intrachain H-aggregation. Previous studies have shown that in semiconducting polymers, H-aggregates are a result of strong intrachain interactions. ⁴² Therefore, it is proposed that these polymers form folded chains and that the movement of charge is through intrachain charge transfer. The extinction coefficient of both polymers at their highest absorption wavelengths and that of the TPTQ acceptor are shown in Table 1. Although the absorptivity is similar for the investigated polymers, TPTQF _C has a slightly higher molar extinction coefficient in the solution. Its molar extinction coefficient at the maximum absorption wavelength (470 nm) is 42505 M⁻¹ cm⁻¹. This slight increase is quite interesting, given that the TPTQ C polymer counterpart has a broadened and red-shifted absorption.

In addition, the absorption spectra of both polymers show well-resolved vibronic transitions. Compared to the TPTQ acceptor absorption, the 0-0 transitions of the polymers are totally different where their 0-0 transition intensity is

significantly reduced, and the 0–1 transition becomes the strongest; this change in the feature intensity indicates the formation of H-aggregates. In addition, there is a significant enhancement of the 0–0 transition peak at 470 nm of TPTQF_C as compared to the 0–0 transition peak of TPTQ_C at 483 nm, indicating stronger aggregation of the TPTQF C polymer chain.

The emission spectra of both polymers and the acceptor, which were obtained in chloroform, are shown in Figure 2b and the relevant data are recorded in Table 1. Structurally, it is clear that the thiophene-based polymer, TPTQ C has an additional emissive peak around 490 nm. The emission spectra of the rigid TPTQF C are blue-shifted compared to that of TPTQ C. A smaller Stokes shift and higher fluorescence quantum yields (Table 1) are observed for TPTQF C as compared to TPTQ_C which may be attributed to the heavy atom effect in TPTQ C. The decreased Stokes shift of TPTQF_C confirms its increased backbone rigidity compared to that of TPTQ_C.5 Compared to both polymers, the fluorescence quantum yield of the TPTQ acceptor is more than two times lower. However, an intense fluorescence in the furan-based polymer (TPTQF C) was observed, which has been associated with decreased intersystem crossing (ISC) due to the lack of the heavier atom, sulfur. Here, the increased fluorescence quantum yield shows enhanced radiative decay pathways. For the TPTQ C polymer, the decreased fluorescence quantum yield has been associated with enhanced nonradiative processes. In all of the investigated materials, a \sim 2% decrease in fluorescence quantum yield is observed upon oxygen purging. This decrease in the fluorescence quantum yield indicates the lack of thermally activated delayed fluorescence activity for all of the molecules.

The concentration dependence of the absorption (Figure S1) measurements was used to check for the existence of polymer aggregate chain formation or polymer folding. For both polymers, a decrease in concentration does not change the shape of the spectra, indicating that the H-aggregates exist even at the level of a single polymer chain (in very low concentrations). This further suggests that the polymer is folded to enhance H-aggregation, leading to intrachain H-aggregation.

In addition to the concentration dependence, temperature-dependent emission measurements were carried out to check the possibility of triplet formation in these molecules through phosphorescence. It has been reported that an increase in temperature induces ISC of a singlet (S1) to triplet (T1) leading to a decrease in fluorescence intensity. Since triplets are usually at lower energies than singlet states, the temperature-dependent emission is usually observed in the near-infrared region. Therefore, these measurements show the presence of phosphorescence and can be used to determine the energies of triplets. As shown in Figure S2, temperature-dependent emission is observed for all of the molecules. For the TPTQ acceptor, two bands are observed, one peaked at 844 nm and

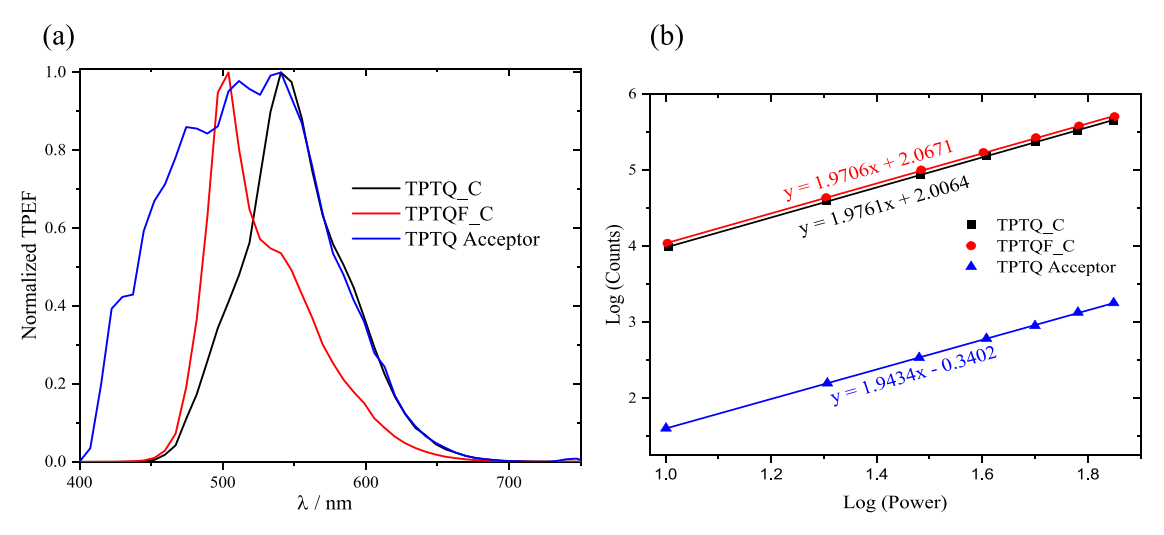


Figure 3. Two photon emission spectra (a) and power dependence of the two photon excited emission (b) of the investigated polymers in chloroform upon 800 nm excitation.

the other one peaked at 906 nm (Figure S2; Table 1). The 844-nm peak decreases in intensity as the temperature of the solution increases from 77 to 273 K. On the contrary, the intensity of the 906-nm peak increases as the temperature increases. Given that high temperatures quench triplet emission, it is safe to assign an 844-nm radius to a triplet state. Therefore, the energy of the TPTQ acceptor triplet is 1.469 eV. For the thiophene-based compound TPTQ_C and the furan-based compound TPTQF_C, the emission band whose intensity decreases as the temperature of their respective solutions increases from 77 to 273 K peaked at 970 and 944 nm, respectively. As such, their triplet energies are 1.28 and 1.31 eV for TPTQ_C and TPTQF_C, respectively.

The results of the two-photon absorption (TPA) crosssection measurements taken at 800 nm with fs pulses are shown in Figure 3. The fluorescence method was used in these experiments. The interesting differences between the three molecules in terms of their cross-section can be observed in Table 1. The TPA cross section for the TPTQF C polymer is 1.3 times more than that of TPTQ C. The TPA cross-section has been directly related to changes in the static and transition dipole moments, which are directly proportional to the charge transfer character of a molecule. 41 Therefore, from the obtained TPA results, TPTQF C has enhanced intrachain charge transfer compared to its thiophene-based analogue (TPTQ C). The increased transition dipole moments in TPTQF C are due to the increased electronegativity of the oxygen atom. These increased transition dipole moments may suggest better interactions between the donor-acceptor junctions, which lead to more efficient charge transfer.

2.2. Time-Resolved Fluorescence Measurements. To understand the fluorescence dynamics of these polymers, time-correlated single photon counting (TCSPC) measurements were carried out. The decay kinetics and the fitted data are shown in Figures 4 and S3, respectively. At the emission maximum, a monoexponential decay function was used to fit the used reference (Coumarin 6), the unpurged and purged spectra of the TPTQ acceptor and the thiophene-based TPTQ_C polymer. However, a biexponential decay function was necessary to fit both the unpurged and purged data of the TPTQF_C polymer. The fluorescence lifetime of the Coumarin 6 reference was found to be 2.8 ns (Table 2)

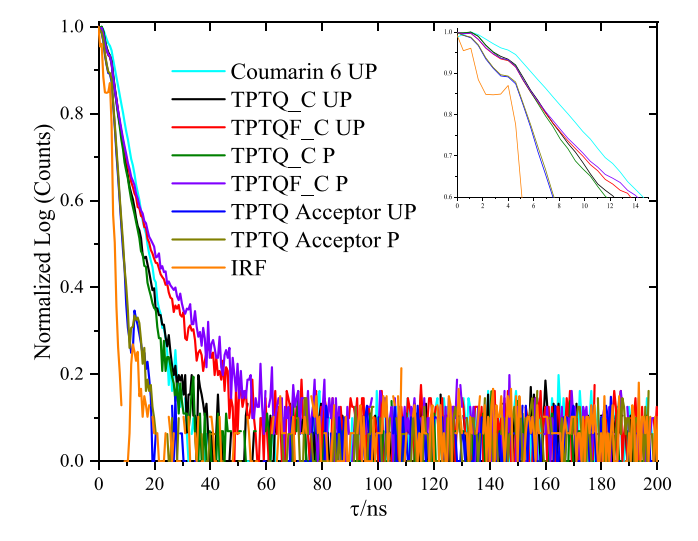


Figure 4. Fluorescence decay lifetimes of the polymers obtained by using time correlated single photon counting experiments. The inset shows the decay dynamics at earlier times.

Table 2. Time Resolved Excited State Lifetime Dynamics of the Investigated Foldable Polymers and the TPTQ Acceptor in Chloroform at the Underlined Wavelengths in Nanoseconds

compound	$\lambda_{\rm em} \ (nm)$	$ au_1$ (UP) (ns)	$ au_2 ext{(UP)} ag{ns)}$	$ au_1$ (P) (ns)	$ au_2$ (P) (ns)
TPTQ acceptor	<u>426</u> , 450, 477	1.3	N/A	1.3	N/A
TPTQ_C	492, <u>548</u> , 600	3.2	N/A	3.2	N/A
TPTQF_C	<u>504</u> , 544	2.9	7.4	2.9	9.0
Coumarin 6		2.8			

which matches very well with the reported 2.4 ns. ⁴³ The two polymers appear to have similar initial time decay dynamics. However, at longer times, the decay of the furan-based polymer slows down midway showing a biexponential decay. At ambient conditions, the τ_1 contribution in the furan-based polymer is 28%, leaving only 72% for τ_2 . However, when oxygen is purged out, the τ_1 contribution drops to 24%, and the τ_2 contribution increases to 76%. Since oxygen has been

reported to quench triplet excitons and with the 25% singlet and 75% triplet exciton rule, the decaying component of the TPTQF_C can be assigned to triplet a species. This contribution is shown by the lifetimes reported in Table 2. For the TPTQ_C polymer, only one species is observed, which decays within 3.2 ns, and its lifetime is not affected by oxygen purging, meaning that this contribution is from the singlet species. However, the TPTQ acceptor, which also decays monoexponentially, decays more than two times faster as compared to the TPTQ_C polymer and the first component of the TPTQF_C polymer as shown in Figure 4 and Table 2.

Interestingly, fluorescence dynamics were also checked at other emitting wavelengths for both polymers (Figure S3). For the furan-based polymer (TPTQF_C), the species at longer wavelengths (542 nm) decays faster compared to those found at the maximum emission peak (504 nm). In the thiophene-based polymer, however, the low-wavelength species decays the fastest. The similarity in decay kinetics between the 498 and 598 nm wavelengths could mean that these are similarly emissive species. However, it is clear that 548 nm species emit differently and can be assigned to different species.

Time-resolved fluorescence upconversion measurements were used to resolve the fast fluorescence of the compounds. As shown in Figure 5, the three compounds have different

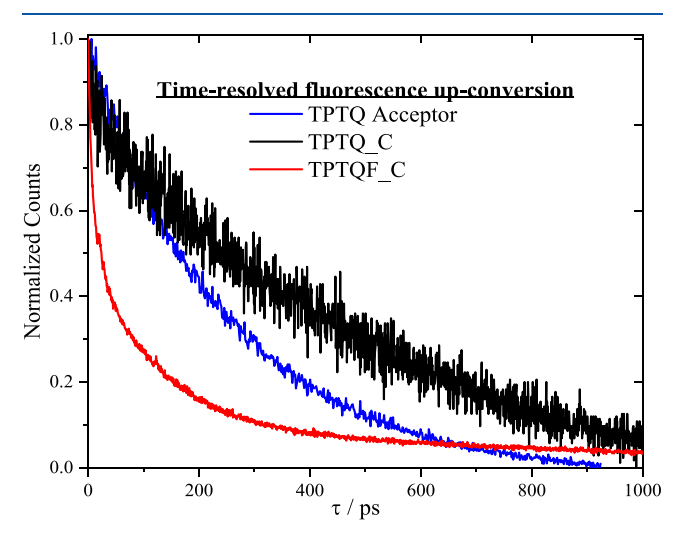


Figure 5. Ultrafast fluoresence upconversion decay kinetics of the investigated polymers obtained using time-correlated single photon counting experiments.

decay dynamics, which were fitted and reported in Table 3. Both polymers fitted well to a triexponential function. The earlier two decay components for both polymers are very fast, however, that of TPTQ_C portrays faster dynamics (4 and 50 ps) compared to the 16 and 205 ps decay time of TPTQF_C. Interestingly, the final and third polymer decay component, which does not necessarily decay completely, shows that

Table 3. Ultrafast Time-Resolved Excited State Lifetime Dynamics of the Investigated Foldable Polymers as well as the TPTQ Acceptor in Chloroform in Picoseconds

compound	λ_{em} (nm)	$\tau_1 \; (ps)$	τ_2 (ps)	τ_3 (ps)
TPTQ acceptor	480	61	264	N/A
TPTQ_C	500	4	50	651
TPTQF_C	500	16	205	280

TPTQF_C decays 2.3 times faster as compared to TPTQ_C. The interesting result showing that the third ultrafast decay component of the decay is faster in TPTQF_C matches well with the results obtained using the TCSPC, where the decay time of the earlier components of the furan-based polymer is faster compared to the thiophene-based counterpart. Therefore, comparing just the polymers, the fluorescence decay results trend obtained using ultrafast upconversion results (later component) matches those obtained using the TCSPC (earlier component). At earlier times, however, the TPTQ acceptor decay time is significantly slower (more than an order of magnitude) than that of both polymer systems. This could indicate that at these earlier times, the polymers are forming a fast species that is not observed in the TPTQ acceptor.

2.3. Transient Absorption Spectroscopy. Both nanosecond and femtosecond transient absorption measurements were used to probe the excited state dynamics of the investigated molecules. The nanosecond transient absorption spectroscopy (nsTAS) measurements were used to probe the long-lived excited state dynamics, while the femtosecond transient absorption spectroscopy (fsTAS) was used to probe the contribution of short-lived states to the photophysics of these materials. The TAS spectra show depletion of the ground state, also known as the ground state bleach (GSB). The excitation of photons to higher excited states can also be observed, which are positive signals called excited state absorption (ESA). A negative signal (stimulated emission-SE) can also be observed when radiative decay happens. For the nsTAS, the compounds were excited using both low (absorption maxima of the respective materials) and high (348) nm) energies, as shown in Figures 6, 7, and S4-S8, and Table 4. All measurements were done at low fluence (~1.2 mJ) excitation. With visible wavelength excitation (483 nm for TPTQ C and 470 nm for TPTQF C), a broad and intense stimulated emission that decays within 100 ns is observed for both polymers (Figure S4a,b). Without the fluorescence background subtraction and exciting at the compounds at their respective maximum absorptions, both polymers show a very small ESA as shown in Figure S5a-d. The peak of these ESAs can be estimated to be ~560 and ~536 nm for TPTQ C and TPTQF C, respectively. The GSBs, whose peak maxima match well with the absorption spectra of the compounds, are observed for both molecules. The observed ESAs are more clearer and less noisy when the compounds are excited using higher energy (348 nm) as shown in Figure 6. The spectra and ESA kinetics of these polymers did not change when the two molecules were excited in UV with the excitation power kept

As shown in Figure 6, a GSB which resembles the one obtained in Figure S5 is observed. The small ESA around 560 nm for TPTQ_C and 536 nm for TPTQF_C becomes more prominent, as shown in Figure 6. For the TPTQ_C compound, the lifetime of the GSB observed at 484 nm increases slightly upon oxygen purging, which may be an indicator of nonsinglet species in the molecule (Figure S6). However, the ESA decay time from this molecule does not change upon oxygen purging, which shows that this ESA is a result of nontriplet species (Figure 7). For the TPTQF_C compound, both the ESA and its GSB are not affected by oxygen purging at all, showing that this ESA is a result of purely singlet states (Figures S6 and 7).

The TPTQ acceptor molecule shows well-resolved dynamics where a GSB with a maximum peak at 420 nm (which matches

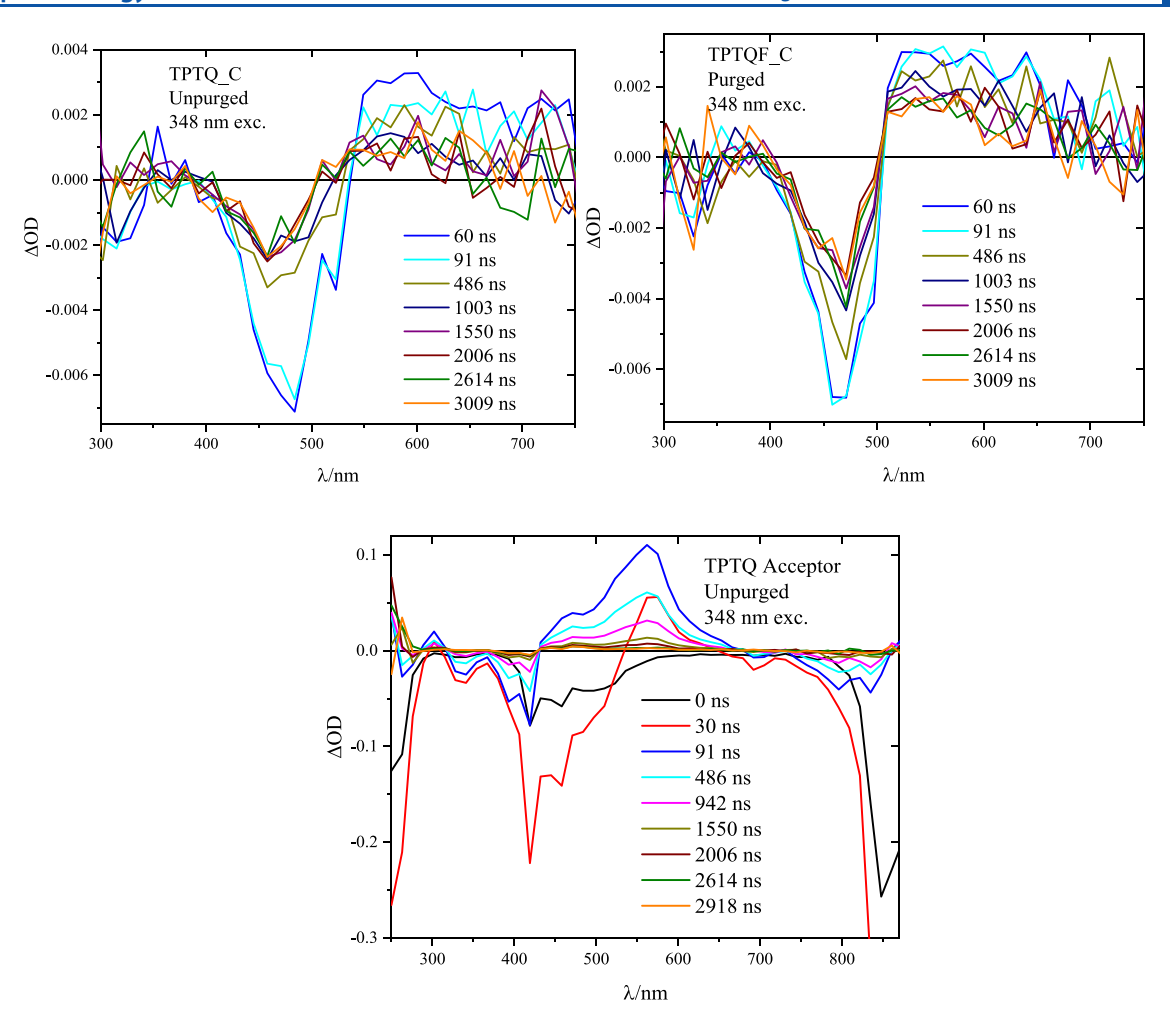


Figure 6. Nanosecond transient absorption spectra of the investigated polymers with a UV excitation of ~2.3 mJ.

well with the ground state absorption) was observed as shown in Figure 6. Two ESA bands are also observed where the ESA at 302 nm decays more slowly as compared to that observed at 562 nm, as shown in Table 4. The lifetimes of both of these ESAs are enhanced upon oxygen purging showing that these ESAs are a result of triplets (Figures 7C and S7). In addition, the GSB decay time is also enhanced by oxygen purging, which further proves the existence of triplet species (Figure S8). Interestingly, there is another GSB peak observed at 844 nm, whose decaytime is also enhanced by oxygen purging (Figure S8). This 844 nm peak matches well with the phosphorescence peak observed in the steady-state studies (Figure S2 and Table 1).

TAS measurements were taken to look into the faster dynamics of the molecules. For both polymer molecules, a GSB that matches well with the respective absorption spectra was observed. At both excitations (respective absorption maxima and 348 nm excitation), the GSB of both polymers forms within 1.00 ps before decaying back slowly (Figures 8 and S9). In both cases, the GSB does not decay completely to zero, which agrees well with the nsTAS results that show long-lived GSB. Additionally, an ESA similar to that observed around the same wavelength range as that for nsTAS was observed for both molecules. For both polymers, the GSB formation and decay happen at the same time as the ESA formation and decay, indicating that the ESA observed is of a

singlet character, which agrees with the nsTAS results. The ESA decay kinetics are shown in Figures S10-S13.

For the TPTQ acceptor, a very intense ESA with two bands was observed. Interestingly, as the ESA at 489 nm decayed, the ESA at 566 nm formed (Figures 8 and S11). This decay and formation, which happens at approximately the same rate, could be connected with the charge transfer of the donor and acceptor species in the system. The ESA at 566 nm is consistent with the ESA observed in the nsTAS measurements and has a decay time of approximately 600 ps. The reason why the singlet species are not observed using the nsTAS is clearly because their decay time is ~600 ps, which is too fast to be resolved by our nsTAS whose instrument response function is only 7 ns. These excited state dynamics measurements with both nanosecond and femtosecond resolution identify the differences in acceptor charge transfer and mobility in comparison to those of the two polymers.

2.4. Electron Paramagnetic Resonance Spectroscopy. As it was predicted that the TPTQ C and TPTQF_C molecules can exist in their resonance states, electron paramagnetic resonance (EPR) spectroscopic measurements were done at ~100 K to check the presence of unpaired electrons in these polymer samples and the TPTQ acceptor. Interestingly, only one of the investigated molecular systems investigated in this study, TPTQ_C, showed a derivative peak where the *g-factor* of the formally forbidden double quantum (nonvertical) transition is ~1.9726 as shown by the green

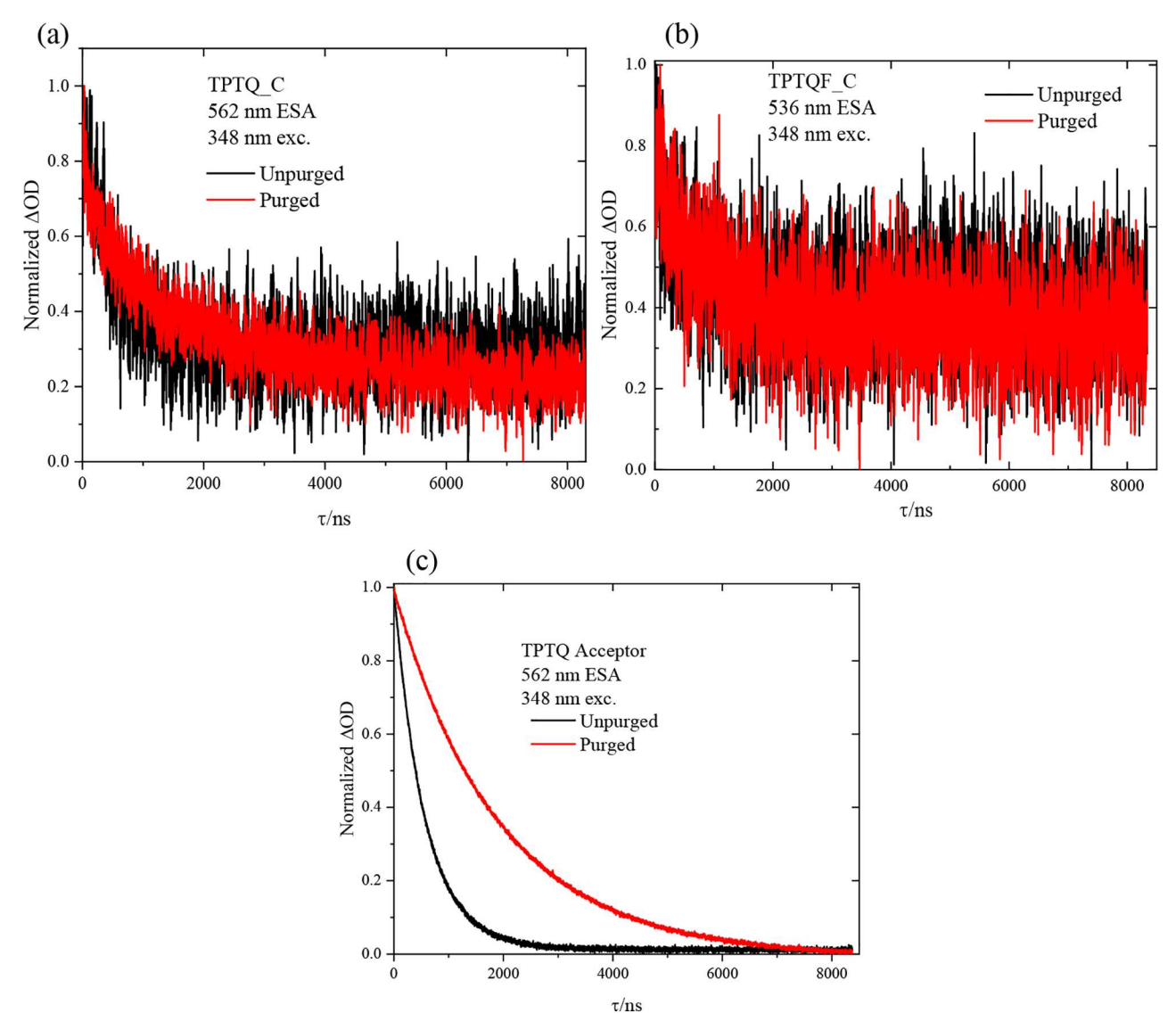


Figure 7. Nanosecond transient absorption ESA kinetics of the investigated polymers with a UV excitation of ~2.3 mJ.

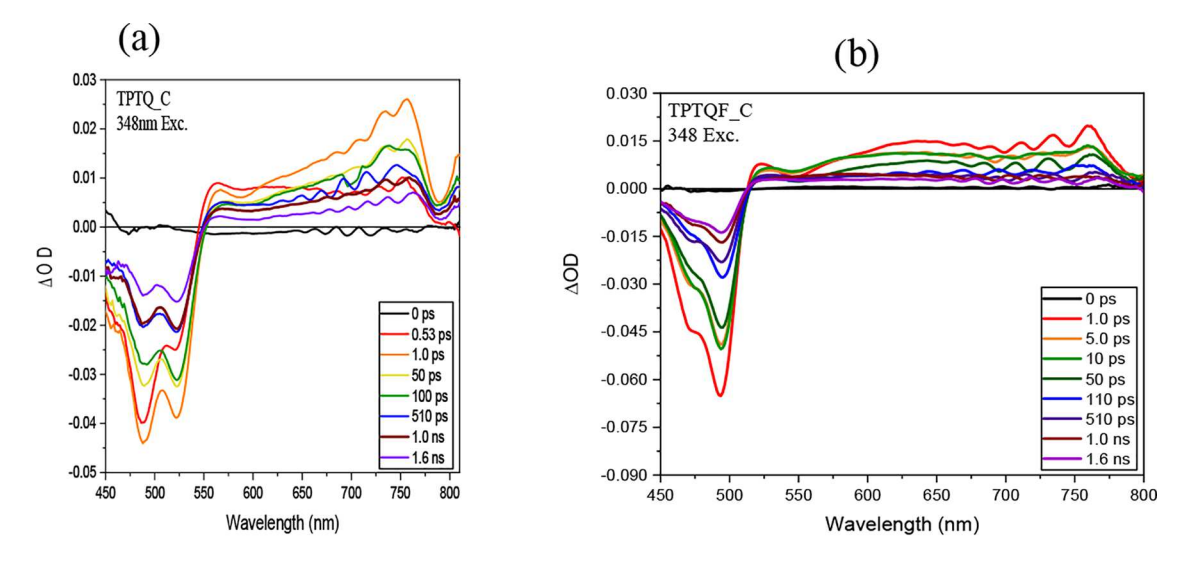
Table 4. Purged (p) and Unpurged (up) nsTAS ESA and GSB Lifetime Dynamics of the Investigated Molecules, as well as the TPTQ Acceptor in Chloroform at Their Indicated Wavelengths

	ESA			GSB					
compound	$\lambda_{\rm em}$ (nm)	$\tau_1(\mathrm{UP}) \; (\mathrm{ns})$	$\tau_1(P)$ (ns)	$\lambda_{\rm em}$ (nm)	$\tau_1(\mathrm{UP}) \; (\mathrm{ns})$	τ_2 (UP) (ns)	$\tau_1(P)$ (ns)	τ ₂ (P) (ns)	
TPTQ acceptor	302	591	2098	420	584	N/A	4415	N/A	
	562	568	1922	844	563	N/A	3793	N/A	
TPTQ_C	562		1164/24,954	484	233	472	214	1294	
TPTQF_C	536		1129/61,214	470	447	801	180	1242	

arrows in the spectra in Figure 9. This *g-factor* shows the presence of organic radicals and has been reported in multiple studies.^{44,45} It is worth noting that there is an additional peak at higher *g-factor* values and a peak at 2.2811. The difference between this peak and the peak derivative is 0.3085. This information is used in the theoretical model described below.

2.5. Quantum Chemical Calculations. The focus of these quantum chemical calculations is on the vertical excitations from the initial structures of the TPTQ acceptor, TPTQ_C, and TPTQF_C. The details of computational methodologies are presented in the SI. The predicted absorption wavelengths are shown in Table 5 and are

consistent with the trend of experimental results (strongest absorption wavelength, TPTQ_C > TPTQF_C > TPTQ acceptor). The natural transition orbitals (NTOs) in Figure 10 indicate charge transfer from the nitrogen to the oxygen, via $\pi \to \pi^*$ excitations in the aromatic rings. In Figure S14, the planarity of the TPTQ acceptor, TPTQ_C, and TPTQF_C, which allows for the different charge transfers, is characterized. The predictions show that TPTQ_C has a smaller HOMO–LUMO bandgap (2.25 eV) as compared to the TPTQF_C (2.38 eV). Incorporating the furan in the electron-deficient material interestingly leads to higher energies for both HOMO (–5.42 eV) and LUMO (–3.04 eV). However, TPTQ_C has



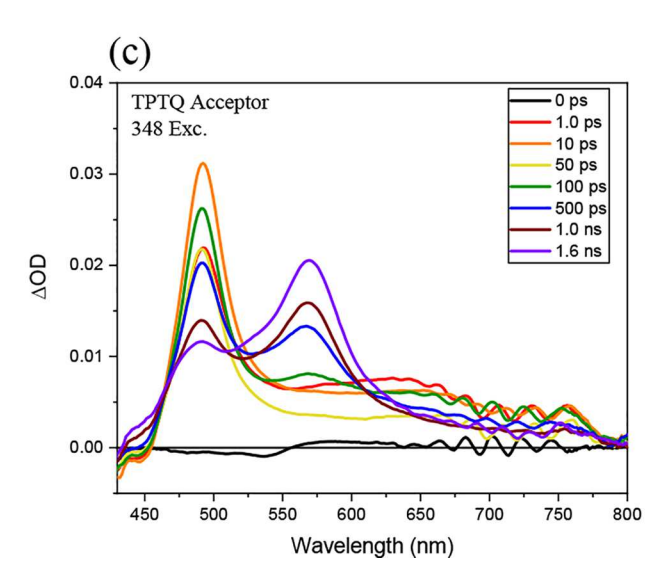


Figure 8. fsTAS spectra of both the TPTQ_C and TPTQF_C polymers as well as the TPTQ acceptor at 348 nm excitation.

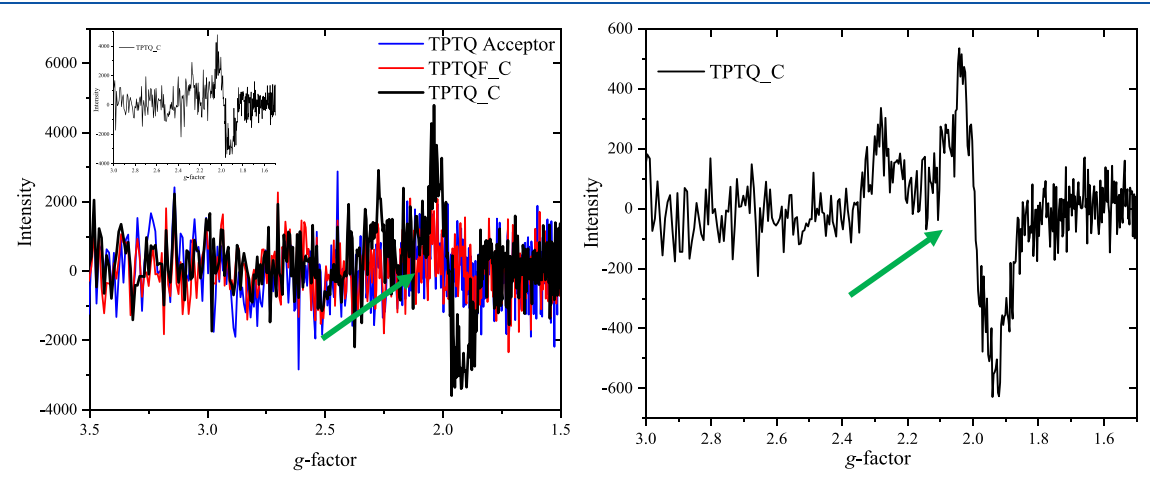


Figure 9. EPR measurements of the investigated molecules. On the right, the TPTQ_C measurements were repeated at a lower concentration.

a slightly lower HOMO (-5.44 eV) and lower LUMO (-3.19 eV). These results indicate there should be a better intrachain charge transfer from the donor to the acceptor of the

TPTQ_C polymer, compared to the charge transfer in TPTQF_C.⁴⁶ The orbital energies of TPTQ_C, TPTQF_C, and the TPTQ acceptor are shown in Table S1. In addition to

Table 5. Absorption Spectra (nm) for TPTQ_C, TPTQF_C, and TPTQ Acceptors from Experiment and Computational Approaches.⁴

$wavelength \ (nm)$	TPTQ_C	TPTQF_C	TPTQ acceptor
$S0 \rightarrow S1$	446 (0.97)	428 (0.93)	419 (0.69)
$S0 \rightarrow T1^{b}$	607 (0.00)	580 (0.00)	578 (0.00)
experiment	455, <u>483</u> , 520	440, <u>470</u> , 489	332, 348, 397, <u>419</u>

"S0, S1, and T1 represent the singlet ground, first singlet excited, and first triplet excited states, respectively. Values in parentheses indicate the oscillator strengths. ^bZero oscillator strength due to no spin—orbit coupling in the calculations.

the HOMO-LUMO energy gap, the singlet/triplet energy gap was also calculated at the Density Functional Theory (DFT) level for TPTQ_C, TPTQF_C, and the TPTQ acceptor. The ground state of each of the calculated structure is a singlet, and the first triplet excited state requires a lot less energy than the first singlet excited state (at least 150 nm lower in energy for the three complexes).

The structures, as well as ground and excited information for both polymers, are illustrated in Figure 11 and Table 6. The isosurface for spin densities of TPTQ_C, TPTQF_C, and acceptor are depicted in Figure S15, showing the diradical electron distribution along the Π systems The carbon—carbon bond distance C—C 3 decreases from the ground to the excited state (1.462–1.437 Å for TPTQ_C and 1.452–1.425 Å for TPTQF_C), which indicates the excited state has a larger weight of the zwitterion resonance form than the ground state.

To characterize the diradical characters of the molecules, the natural orbital occupation number (NOON) of the ground and excited states of TPTQ_C, TPTQF_C, and TPTQ acceptor were evaluated and presented in Table 7. This same method has been used and reported in the literature. The Mulliken spin densities presented in Figure 12 indicate the spatial locations of spin-polarized electrons.

The unrestricted Hartee–Fock (UHF) NOON values obtained theoretically were used to compute the diradical character, y, of all the investigated materials based on a method previously described by Kamada et al. Here, the diradical resonance contribution to the ground structure, also known as the singlet diradical character index, y, is calculated from using the Hartee–Fock method where

$$y = 1 - \frac{2T}{1 + T^2} \tag{1}$$

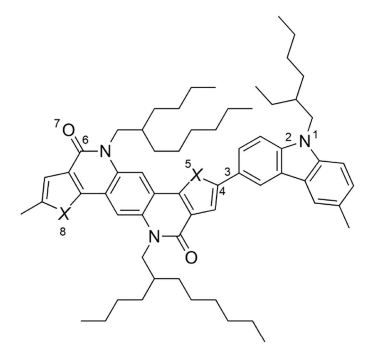


Figure 11. Structure for TPTQ C (X=S) and TPTQF C (X=O).

T is represented using the occupational numbers of (n) of UHF natural orbitals

$$T = \frac{n_{\text{HOMO}} - n_{\text{LUMO}}}{2} \tag{2}$$

3. DISCUSSION

In this study, the photophysical properties are reported of previously synthesized semiladder polymers consisting of two different acceptor monomers: thienopyridothienoquinoline, which has a thiophene incorporated (TPTQ_C) and thienopyridothienoquinoline with a furan molecule incorporated (TPTQF C). Both of these acceptors are coupled to a carbazole donor monomer moiety. Previous reports have shown the photoinduced radical polymerization of quinolines through intramolecular charge transfer that cleaves certain C-O bonds to form radicals. 49 Elsewhere, carbazole-donor-based fullerene polymers have been reported to form long-lived singlet diradicals upon light absorption. 50 In some molecules, these diradicals can transition to form long-lived zwitterions.²⁶ To the best of our knowledge, no one has reported timeresolved and nonlinear optical properties and the charge transfer mechanism that involves the formation of diradicaloids in foldable ladder-type polymer aggregates for OLET applications. Thus, from our studies, we propose that the diradicaloids formed in the case of the TPTQ C molecule reduce the charge and energy transfer rate of the thiophenecarbazole-based OLET polymers. The reduced energy transfer process leads to a decreased overall (EQE) of the resultant OLETs with diradicaloid character.

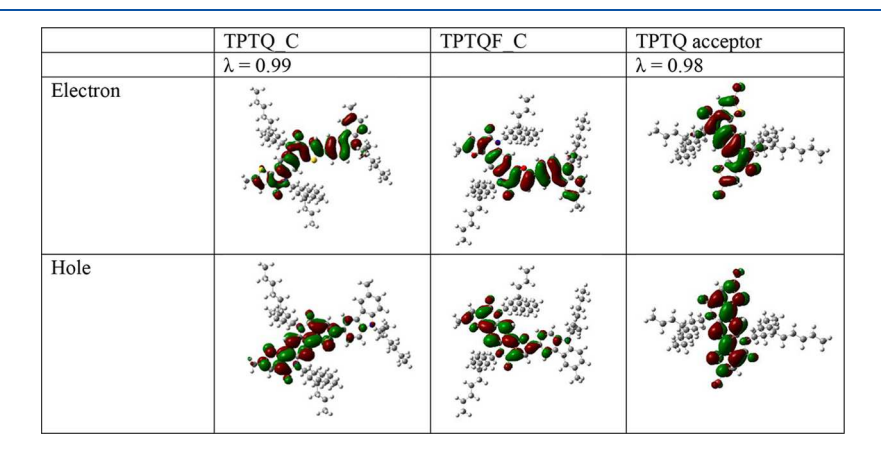


Figure 10. NTOs for TPTQ C, TPTQF C, and TPTQ acceptors. λ indicates the eigenvalue of the transition.

Table 6. Partial Natural Population Analysis Charges (Atomic Unit) and Bond Distances (Å) in the Ground and Excited States of TPTQ C and TPTQF_C

		N1	C4	X5	O7	X8	N1-C 2	C3-C4	C6-O 7
TPTQ_C	S0	-0.386	-0.177	0.443	-0.628	0.439	1.386	1.462	1.231
	S1	-0.345	-0.211	0.392	-0.632	0.404	1.379	1.437	1.234
TPTQF_C	S0	-0.483	0.374	-0.550	-0.735	-0.553	1.385	1.452	1.229
	S1	-0.384	0.322	-0.457	-0.626	-0.460	1.378	1.425	1.234

Table 7. Diradical Character of TPTQ_C, TPTQF_C, and TPTQ Acceptor, Characterized by the UHF Spin Value $\langle S^2 \rangle$ and NOON

	TPTQ_C	TPTQF_C	TPTQ acceptor
ground state (S0) $\langle S^2 \rangle$	2.68	2.54	1.46
ground state (S0) NOON	1.64, 0.36	1.66, 0.34	1.68, 0.32
excited state (S1) NOON	1.22, 0.75	1.25, 0.73	1.04, 0.98
computed diradical character, y (ground state (S0) NOON)	0.09	0.08	0.07
computed diradical character y', (excited state (S1) NOON)	0.55	0.51	0.94

From the steady-state absorption, and just considering the maximum absorption (Figure 2; Table 1), it is clear that TPTQ_C has a slightly lower HOMO–LUMO bandgap (2.567 eV) compared to the TPTQF_C (2.638 eV). Here, the HOMO–LUMO bandgap of the furan-based polymer is 0.071 eV higher than the generally suggested difference of 0.3–0.4 eV.⁵¹ The weak low-energy shoulder observed at 520 nm has been reported to originate from low-lying singlet states, which are mostly because of doubly excited electronic configuration (HH/LL) and indicate the presence of open-shell singlet ground states in the form of diradicaloids. ^{23,31,52–54} This weak and low-energy shoulder is the first evidence that shows the

presence of diradical character in only the TPTQ_C molecule and backed-up by its lowest HOMO–LUMO bandgap. The red-shifted emission of the TPTQ_C compound can also be attributed to its larger diradical character and has been reported to improve the electron delocalization and the compound's diradical resonance, effectively reducing their optical energy gaps.²⁴

Additionally, the faster fluorescence decay kinetics, as well as lower fluorescence quantum yield, indicates fluorescence quenching in the thiophene-based polymer (TPTQ C) compared to its counterpart TPTQF C. This quenching can be associated with increased molecular aromatization and conjugation which increases the fluorophores density. 55 Due to its high aromatic stability, TPTQ C can form neutral zwitterions through the cleaving of the C=O in the thiophene acceptor, followed by an electronic reorganization to form a cation on the amine side of the carbazole donor. This cation formation can be followed by self-doping leading to the formation of diradicals.³³ However, the presence of furan in TPTQF C reduces its aromaticity and increases the quinoidal interactions, which inhibit the diradical formation. Similar results were observed by Xue et al. and Sander.^{23,56} As mentioned above, low fluorescence quantum yields have been reported for materials with increased diradical character. 52

Figure 12. Mulliken spin densities for TPTQ_C, TPTQF_C, and the TPTQ acceptor. Absolute values greater than 0.3 are labeled near the associated atoms.

Table 8. Calculated Diradical Character, y, ΔE_{ST} , and J from the Steady-State Measurements

compound	$l_{S_{1u}S_{1g}}$ (nm)	$E_{S_{1u}S_{1g}}$ (eV)	$l_{T_{1u}S_{1g}}$ (nm)	$E_{T_{1u}S_{1g}}\left(\mathrm{eV}\right)$	$l_{S_{2g,S1g}}$ (nm)	$E_{S_{2g,S1g}}$ (eV)	у	$\Delta E_{ m ST}$	J
TPTQ acceptor	419	2.9541	844	1.469	540	4.592	0.053	1.485	0.74
TPTQ_C	522	2.375	970	1.278	600	2.296	0.122	1.097	0.55
TPTQF_C	496	2.500	944	1.313	540	4.592	0.034	1.186	0.59

$$A + D \leftrightarrow A^{-} + D^{+} \leftrightarrow A^{\cdot} + D^{\cdot} \tag{3}$$

Given the reported steady-state results, a few parameters were obtained to calculate the singlet diradical character, *y*, of the investigated materials using the expression (eq 4) derived and reported by Kamada et al.⁵⁷

$$y = 1 - \sqrt{1 - \left(\frac{E_{S_{1u}S_{1g}} - E_{T_{1u}S_{1g}}}{E_{S_{2g,S_{1g}}}}\right)^2}$$
 (4)

where $E_{S_{1u}S_{1g}}$ is given by the lowest energy peak of the one-photon absorption spectra, $E_{T_{1u}S_{1g}}$ is obtained from phosphorescence peak measurements and $E_{S_{2g},S_{1g}}$ corresponds to the lowest energy peak of the TPA spectra. Based on these steady-state parameters, the calculated diradical character shows an element of diradical character in these molecules with the TPTQ_C molecule showing the largest y (Table 8).

Additionally, the singlet—triplet energy gap ($\Delta E_{\rm ST}$) was calculated by subtracting the triplet state energy ($E_{\rm T}$) from the singlet state energy ($E_{\rm S}$). Here, TPTQ_C shows a lower $\Delta E_{\rm ST}$ bandgap compared to TPTQF_C. Previous studies have used the singlet—triplet energy gap of diradicaloids to not only rule out the possibility of biradical formation but also determine the spin multiplicity of the diradicals. Su et al. report that the diradicaloids can be characterized by a positive electron exchange interaction, J, which means that there is some level of coupling between the nonbonding electrons, as shown in eq 5. 58

$$\Delta E_{ST} = E_S - E_T = 2J \tag{5}$$

The presence of electron exchange interaction indicates that there is some coupling between the nonbonding electrons, which eliminates the possibility that the nonbonding electrons could be forming diradicals instead of biradicals.

The diradical character in TPTQ_C is also ascertained by the signal observed in the EPR measurements. The appearance of the EPR spectra observed in our results can be explained by the forbidden $\Delta ms = \pm 2$ EPR transitions which become weakly allowed by the second-order perturbation in the zero-field splitting Hamiltonian to produce distinct states. The intensity of the half-field transitions is therefore much weaker, as shown at 3167G and 3514G (Figure 13). The EPR allowed transitions of the TPTQ_C molecule lead to degenerate E_x and E_y . As a result, E_x and E_y = 3241G while E_z = 3167G. This information can be used to calculate the zero-field splitting parameters, E and E_y and E_y = 74G, E_y = 148G. Since E_y = 49.3G. The experimentally computed E_y parameter can therefore be used to determine the spin—spin distance E_y using eq 6 below.

$$D = 1.39X10^4 (g/r^2) (6)$$

where:

g = g-factor and

r is the spin-spin distance.

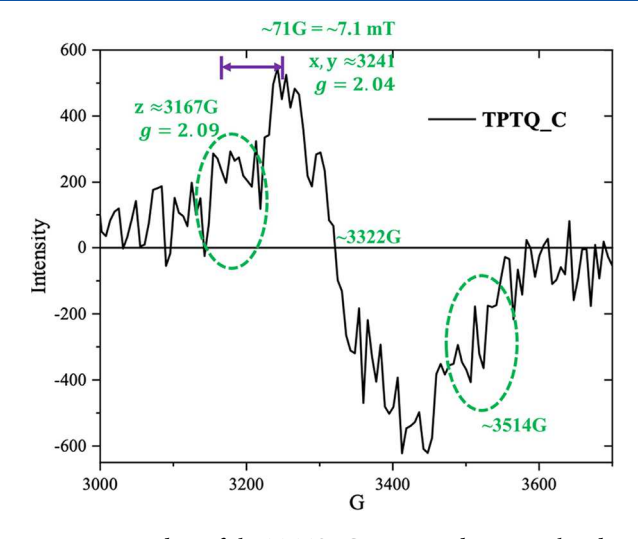


Figure 13. EPR data of the TPTQ_C compound were analyzed.

From the above equation, the spin–spin distance, r, is 5.8 Å. This calculated spin–spin distance is smaller than the previously reported spin–spin distance between two non-bonding electrons (6.4 Å) of a stable diradical emitter. ⁶⁰

From the transient absorption, the positive ESA, which, according to fsTAS, has a growth and decay time equivalent to that of their respective ground state depletion, is assigned to singlet states. This assignment to singlet states is further reinforced by the nsTAS measurements, where the ESA lifetimes are not enhanced in nitrogen-rich environments. Surprisingly, lifetimes of these ESAs are beyond the usual singlet state lifetimes of a couple of 10-100 ns. Here, we obtain 25 and 60 µs for TPTQ C and TPTQF C, respectively. The TPTQ C ESA is assigned to diradicaloids. These long lifetime diradicaloid species whose lifetime is affected by purging out oxygen have been reported in previous studies.⁶¹ We suggest that for TPTQF_C, the long-lived singlet state is as a result of zwitterions states which have been reported to appear in higher energies than diradical states.²⁵ Based on our experimental data, we propose the energy level diagram shown in Figure 14.

The Mulliken spin density in Figure 12 suggests all three systems are more similar to diradicals rather than biradicals, namely, the polarized electrons are not located in two spatial centers. To compare the diradical characters among TPTQ_C, TPTQF_C, and TPTQ acceptor, the values of $\langle S^2 \rangle$ and NOON in Table 5 were estimated. Larger $\langle S^2 \rangle$ and deviations from the values 2.0 and 0.0 suggest stronger diradical character. The $\langle S^2 \rangle$ and NOON in Table 7 indicate that TPTQ_C and TPTQF_C have significant diradical character, both of which are stronger than that of TPTQ acceptor. This may be explained by TPTQ_C and TPTQF_C having more extended conjugated ranges than the acceptor, similar to the increasingly large diradical characters observed in higher-order acenes. TPTQ_C exhibits a slightly larger diradical character than TPTQF_C ($\langle S^2 \rangle$ are 2.68 and

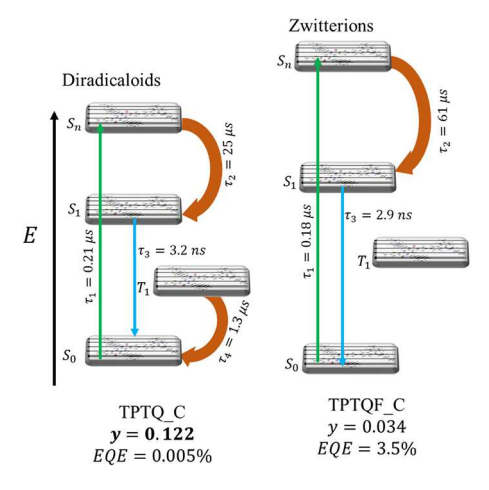


Figure 14. Proposed energy level diagram for the diradicaloids observed for TPTQ_C and the zwitterions formed in the case of the TPTQF_C.

2.54 for TPTQ_C and TPTQF_C, respectively). This may be explained by the fact that the atomic orbital energy of sulfur 3p (-0.263 hartree) is closer to carbon 2p (-0.199 hartree) than oxygen 2p (-0.338 hartree) is to carbon 2p (-0.199 hartree).

From previous studies^{5,13,17} it is possible for quinoline derivatives like TPTQ C and TPTQF C to exist in their resonant forms as shown in Figure 1. Due to the presence of sulfur, the thiophene-based polymer resonant structure becomes more unreactive due to its high aromatic stability compared to the furan-based counterparts. The TPTQF C, which is more reactive, is extremely unstable, and its resonant structure is very short-lived. Similar results were reported by Jursic where sulfur heterocyclic compounds showed the highest resonance stability while their furan derivatives were the most reactive.⁶³ Previous polymer studies show that furan has reduced aromaticity which increases the contribution from quinoidal resonance structure in polyfurans making furancontaining polymers more rigid with a planar conformation as well as an overly increased conjugation. 18 This decrease in aromaticity around the furan moiety tends to enhance the probability of additional reactions like that of singlet oxygen and light, compared to their counterpart thiophene-based polymers. ¹⁸ This is an interesting observation since previously, a decrease in aromaticity has been related to an increase in the diradical character of molecules. 64,65 The saturation of this π conjugation leads to an unexpected shift of the absorption maximum to high energies. However, the lone pair of electrons on the sulfur atom in the TPTQ $_C$ polymer leads to $p-\pi$ conjugation, extending the overall conjugation of the thiophene-based TPTQ _C polymer. This extended conjugation leads to intensified absorption, which is shifted to longer wavelengths as confirmed by the TPTQ C absorption in Figure 2a.

4. CONCLUSIONS

The presence of unpaired electrons in an open-shell molecule has been reported to form resonant structures with the enhanced spin density that is delocalized along the planar π -conjugated backbone, influencing charge transfer. The existence of degenerate or nearly degenerate nonbonding orbitals containing radicals can offer intermolecular spin—spin interactions, which lead to σ -aggregation and formation of σ -

polymerization, affecting intermolecular stacking and charge transport, proving to be good for OLEDs. Per our experimental work, we believe that the thiophene-based compound (TPTQ_C) displays a diradical character. This conclusion is suggested as a result of a number of properties. First, the weak low-energy shoulder observed at 520 nm has been reported to originate from low-lying singlet states which are mostly a result of doubly excited electronic configuration (HH/LL) and indicate the presence of open-shell singlet ground states in the form of diradicaloids. Second, fluorescence quenching in the polymer along with the low fluorescence quantum yields and lower TPA cross-section suggest an increased diradical character. 54,66 Third, based on the optical and calculated diradical character (y) results, the TPTQ C molecule has the largest diradical character. In addition, the calculation of the electron exchange interaction parameter shows that there is some interaction between the two unpaired electrons, which means that the open-shell structure formed is of diradical character and not biradical. Fourth, TPTQ C has the lowest singlet-triplet energy gap (ΔE_{ST}). Fifth, a signal is observed from EPR measurements with a g-factor of ~2.000, which is typical of organic radicals. And sixth, the unusually long-lived ESA (25 μ s) with a singlet character that was observed for the TPTQ C compound has also been reported in other rylene diradical states and is assigned to the singlet diradicaloid states for this compound. These results strongly point to the diradical character of the TPTQ-C molecule and will be useful in the design of new and highly efficient OLET devices.

ASSOCIATED CONTENT

Supporting Information

The Supporting Information is available free of charge at https://pubs.acs.org/doi/10.1021/acsaem.4c00685.

Experimental details of the time-resolved fluorescence and fs transient absorption measurements as well as quantum chemical calculations (PDF)

AUTHOR INFORMATION

Corresponding Author

Theodore G. Goodson, III — Department of Chemistry, University of Michigan, Ann Arbor, Michigan 48109, United States; orcid.org/0000-0003-2453-2290; Email: tgoodson@umich.edu

Authors

Angelar K. Muthike — Department of Chemistry, University of Michigan, Ann Arbor, Michigan 48109, United States

Mohammad Ahmad Awais — Department of Chemistry and The James Franck Institute, The University of Chicago, Chicago, Illinois 60637, United States

Cong Wang — Department of Chemistry, Michigan State University, East Lansing, Michigan 48864, United States Meghan E. Orr — Department of Chemistry, University of Michigan, Ann Arbor, Michigan 48109, United States

Nuno M.S. Almeida – Department of Chemistry, Michigan State University, East Lansing, Michigan 48864, United States; ocid.org/0000-0002-6091-7289

Sasha C. North — Department of Chemistry, Michigan State University, East Lansing, Michigan 48864, United States; orcid.org/0000-0002-2877-592X

Luping Yu — Department of Chemistry and The James Franck Institute, The University of Chicago, Chicago, Illinois 60637, United States

Angela K. Wilson — Department of Chemistry, Michigan State University, East Lansing, Michigan 48864, United States; orcid.org/0000-0001-9500-1628

Complete contact information is available at: https://pubs.acs.org/10.1021/acsaem.4c00685

Notes

The authors declare no competing financial interest.

ACKNOWLEDGMENTS

T.G.III acknowledges support from the National Science Foundation through (CHE-2004076), the Air Force Office of Scientific Research (Biophysics no. FA9550-20-1-0380), and the U.S. Department of Energy, Office of Science, Office of Basic Energy Sciences under award DE-SC0022118. A.K.W. gratefully acknowledges support by the U.S. Department of Energy (DOE) Office of Science (Office of Basic Energy Science) under grant DE-SC0017889 as well as from MSU for the support of a John A. Hannah Professorship. Yu thanks the support of NSF (CHE-2102102). The authors gratefully acknowledge computational resources from the iCER computational facility at Michigan State University.

REFERENCES

- (1) Hepp, A.; Heil, H.; Weise, W.; Ahles, M.; Schmechel, R.; von Seggern, H. Light-Emitting Field-Effect Transistor Based on a Tetracene Thin Film. *Phys. Rev. Lett.* **2003**, *91* (15), No. 157406.
- (2) Liu, C. F.; Liu, X.; Lai, W. Y.; Huang, W. Organic Light-Emitting Field-Effect Transistors: Device Geometries and Fabrication Techniques. *Adv. Mater.* **2018**, *30*, No. 1802466.
- (3) Yuan, D.; Sharapov, V.; Liu, X.; Yu, L. Design of High-Performance Organic Light-Emitting Transistors. *ACS Omega* **2020**, *5*, 68–74.
- (4) Ojha, S. K.; Kumar, B. Parameter Extraction of High-Performance Material Based Organic Light-Emitting Transistors (OLETs). *Silicon* **2022**, *14*, 3999.
- (5) Yuan, D.; Awais, M. A.; Sharapov, V.; Liu, X.; Neshchadin, A.; Chen, W.; Bera, M.; Yu, L. Foldable Semi-Ladder Polymers: Novel Aggregation Behavior and High-Performance Solution-Processed Organic Light-Emitting Transistors. *Chem. Sci.* **2020**, *11* (41), 11315–11321.
- (6) Chen, H.; Xing, X.; Miao, J.; Zhao, C.; Zhu, M.; Bai, J. W.; He, Y.; Meng, H. Highly Efficient Flexible Organic Light Emitting Transistor Based on High-k Polymer Gate Dielectric. *Adv. Opt Mater.* **2020**, *8* (6), No. 1901651.
- (7) Yuan, D.; Awais, M. A.; Sharapov, V.; Liu, X.; Neshchadin, A.; Chen, W.; Yu, L. Synergy between Photoluminescence and Charge Transport Achieved by Finely Tuning Polymeric Backbones for Efficient Light-Emitting Transistor. *J. Am. Chem. Soc.* **2021**, *143* (13), 5239–5246.
- (8) Feldmeier, E. J.; Schidleja, M.; Melzer, C.; Von Seggern, H. A Color-Tuneable Organic Light-Emitting Transistor. *Adv. Mater.* **2010**, 22 (32), 3568–3572.
- (9) Soldano, C. Engineering Dielectric Materials for High-Performance Organic Light Emitting Transistors (Olets). *Materials* **2021**, *14* (13), 3756.
- (10) Feng, G.; Xu, Y.; Xiao, C.; Zhang, J.; Zhang, X.; Li, C.; Wei, Z.; Hu, W.; Wang, Z.; Li, W. Poly(Pentacyclic Lactam-Alt-Diketopyrrolopyrrole) for Field-Effect Transistors and Polymer Solar Cells Processed from Non-Chlorinated Solvents. *Polym. Chem.* **2016**, 7 (1), 164–170.
- (11) Tanaka, H.; Kajii, H.; Ohmori, Y. Effects of Molecular Packing on the Field-Effect Mobility and External Quantum Efficiency of

- Ambipolar Polymer Light-Emitting Transistors Incorporating a Donor-Acceptor Polymer. Synth. Met. 2015, 203, 10–15.
- (12) Qin, Z.; Gao, H.; Liu, J.; Zhou, K.; Li, J.; Dang, Y.; Huang, L.; Deng, H.; Zhang, X.; Dong, H.; Hu, W. High-Efficiency Single-Component Organic Light-Emitting Transistors. *Adv. Mater.* **2019**, *31* (37), No. 1903175.
- (13) Zheng, C.; Zhong, C.; Collison, C. J.; Spano, F. C. Non-Kasha Behavior in Quadrupolar Dye Aggregates: The Red-Shifted H-Aggregate. *J. Phys. Chem. C* **2019**, *123* (5), 3203–3215.
- (14) Kelley, R. F.; Rybtchinski, B.; Stone, M. T.; Moore, J. S.; Wasielewski, M. R. Solution-Phase Structure of an Artificial Foldamer: X-Ray Scattering Study. *J. Am. Chem. Soc.* **2007**, *129* (14), 4114–4115
- (15) Hu, X.; Lindner, J. O.; Würthner, F. Stepwise Folding and Self-Assembly of a Merocyanine Folda-Pentamer. *J. Am. Chem. Soc.* **2020**, 142 (7), 3321–3325.
- (16) Fauvell, T. J.; Zheng, T.; Jackson, N. E.; Ratner, M. A.; Yu, L.; Chen, L. X. Photophysical and Morphological Implications of Single-Strand Conjugated Polymer Folding in Solution. *Chem. Mater.* **2016**, 28 (8), 2814–2822.
- (17) Terenziani, F.; Painelli, A.; Katan, C.; Charlot, M.; Blanchard-Desce, M. Charge Instability in Quadrupolar Chromophores: Symmetry Breaking and Solvatochromism. *J. Am. Chem. Soc.* **2006**, 128 (49), 15742–15755.
- (18) Cao, H.; Rupar, P. A. Recent Advances in Conjugated Furans. *Chem.—Eur. J.* **2017**, 23 (59), 14670–14675.
- (19) Sergeants-and-Soldiers Principle in Chiral Columnar Stacks of Disc-Shaped Molecules with C3 Symmetry.
- (20) Nelson, J. C.; Saven, J. G.; Moore, J. S.; Wolynes, P. G. Solvophobically Driven Folding of Nonbiological Oligomers; Plenum, 1995; Vol. 267. https://www.science.org.
- (21) Håheim, K. S.; Urdal Helgeland, İ. T.; Lindbäck, E.; Sydnes, M. O. Mapping the Reactivity of the Quinoline Ring-System Synthesis of the Tetracyclic Ring-System of Isocryptolepine and Regioisomers. *Tetrahedron* **2019**, *75* (21), 2949–2957.
- (22) Hosmane, R. S.; Liebman, J. F. Paradoxes and Paradigms: Why Is Quinoline Less Basic than Pyridine or Isoquinoline? A Classical Organic Chemical Perspective. *Struct Chem.* **2009**, 20 (4), 693–697.
- (23) Xue, G.; Hu, X.; Chen, H.; Ge, L.; Wang, W.; Xiong, J.; Miao, F.; Zheng, Y. Understanding the Nature of Quinoidal and Zwitterionic States in Carbazole-Based Diradicals. *Chem. Commun.* **2020**, *56* (38), 5143–5146.
- (24) Chen, L. M.; Lin, I. H.; You, Y. C.; Wei, W. C.; Tsai, M. J.; Hung, W. Y.; Wong, K. T. Substitution Effect on Carbazole-Centered Donors for Tuning Exciplex Systems as Cohost for Highly Efficient Yellow and Red OLEDs. *Mater. Chem. Front* **2021**, *5* (13), 5044–5054.
- (25) Chesta, C. A.; Whitten, D. G. Photocyclization Of-Keto Amides in Homogeneous Solution and Aqueous Cyclodextrin Media. The Role of Zwitterions and Diradicals in Photoinduced Electron Transfer Reactions. J. Am. Chem. Soc. 1992, 114, 2188.
- (26) Piotrowiak, P.; Strati, G.; Smirnov, S. N.; Warman, J. M.; Schuddeboom, W. Singlet Biradical to Singlet Zwitterion Optical Transition in a Twisted Olefin. *J. Am. Chem. Soc.* **1996**, *118*, 8981–8982
- (27) Bendikov, M.; Duong, H. M.; Starkey, K.; Houk, K. N.; Carter, E. A.; Wudl, F. Oligoacenes: Theoretical Prediction of Open-Shell Singlet Diradical Ground States. *J. Am. Chem. Soc.* **2004**, *126* (24), 7416–7417.
- (28) Abe, M. Diradicals. Chem. Rev. 2013, 11, 7011-7088.
- (29) Li, Y.; Li, Y.; Li, L.; Wu, Y. A Review on the Origin of Synthetic Metal Radical: Singlet Open-Shell Radical Ground State? *J. Phys. Chem. C* **2017**, *121* (15), 8579–8588.
- (30) Yuen, J. D.; Wang, M.; Fan, J.; Sheberla, D.; Kemei, M.; Banerji, N.; Scarongella, M.; Valouch, S.; Pho, T.; Kumar, R.; Chesnut, E. C.; Bendikov, M.; Wudl, F. Importance of Unpaired Electrons in Organic Electronics. *J. Polym. Sci. A Polym. Chem.* **2015**, 53 (2), 287–293.
- (31) Kamada, K.; Fuku-En, S. I.; Minamide, S.; Ohta, K.; Kishi, R.; Nakano, M.; Matsuzaki, H.; Okamoto, H.; Higashikawa, H.; Inoue,

- K.; Kojima, S.; Yamamoto, Y. Impact of Diradical Character on Two-Photon Absorption: Bis(Acridine) Dimers Synthesized from an Allenic Precursor. *J. Am. Chem. Soc.* **2013**, *135* (1), 232–241.
- (32) Cui, Z.; Ye, S.; Wang, L.; Guo, H.; Obolda, A.; Dong, S.; Chen, Y.; Ai, X.; Abdurahman, A.; Zhang, M.; Wang, L.; Li, F. Radical-Based Organic Light-Emitting Diodes with Maximum External Quantum Efficiency of 10.6%. *J. Phys. Chem. Lett.* **2018**, 9 (22), 6644–6648.
- (33) Tang, H.; Liu, Z.; Tang, Y.; Du, Z.; Liang, Y.; Hu, Z.; Zhang, K.; Huang, F.; Cao, Y. Organic Diradicals Enabled N-Type Self-Doped Conjugated Polyelectrolyte with High Transparency and Enhanced Conductivity. *Giant* 2021, 6, No. 100053.
- (34) Nagami, T.; Okada, K.; Miyamoto, H.; Yoshida, W.; Tonami, T.; Nakano, M. Molecular Design Principle for Efficient Singlet Fission Based on Diradical Characters and Exchange Integrals: Multiple Heteroatom Substitution Effect on Anthracenes. *J. Phys. Chem. C* 2020, 124 (22), 11800–11809.
- (35) Zeng, Z.; Shi, X.; Chi, C.; López Navarrete, J. T.; Casado, J.; Wu, J. Pro-Aromatic and Anti-Aromatic π -Conjugated Molecules: An Irresistible Wish to Be Diradicals. *Chem. Soc. Rev.* **2015**, *44*, 6578–6596.
- (36) Zong, C.; Zhu, X.; Xu, Z.; Zhang, L.; Xu, J.; Guo, J.; Xiang, Q.; Zeng, Z.; Hu, W.; Wu, J.; Li, R.; Sun, Z. Isomeric Dibenzoheptazethrenes for Air-Stable Organic Field-Effect Transistors. *Angewandte Chemie International Edition* **2021**, *60* (29), 16230–16236.
- (37) Yuan, D. Stable N-Doped Conductors Enabled by Organic Diradicals. *Chem.* **2019**, 5 (4), 744–745.
- (38) Dong, S.; Li, Z. Recent Progress in Open-Shell Organic Conjugated Materials and Their Aggregated States. *J. Mater. Chem. C Mater.* **2022**, *10*, 2431.
- (39) Ai, X.; Evans, E. W.; Dong, S.; Gillett, A. J.; Guo, H.; Chen, Y.; Hele, T. J. H.; Friend, R. H.; Li, F. Efficient Radical-Based Light-Emitting Diodes with Doublet Emission. *Nature* **2018**, *563* (7732), 536–540.
- (40) Miao, J.; Meng, B.; Liu, J.; Wang, L. An A-D-A'-D-A Type Small Molecule Acceptor with a Broad Absorption Spectrum for Organic Solar Cells. *Chem. Commun.* **2018**, *54* (3), 303–306.
- (41) Wang, M.; Wang, H.; Yokoyama, T.; Liu, X.; Huang, Y.; Zhang, Y.; Nguyen, T. Q.; Aramaki, S.; Bazan, G. C. High Open Circuit Voltage in Regioregular Narrow Band Gap Polymer Solar Cells. *J. Am. Chem. Soc.* **2014**, *136* (36), 12576–12579.
- (42) Spano, F. C. The Spectral Signatures of Frenkel Polarons in H-And J-Aggregates. *Acc. Chem. Res.* **2010**, 43 (3), 429–439.
- (43) Eggeling, C.; Brand, L.; Seidel, C. Laser-Induced Fluorescence of Coumarin Derivatives in Aqueous Solution: Photochemical Aspects for Single Molecule Detection. *Bioimaging* **1997**, *5* (3), 105–115.
- (44) Jezierski, A.; Czechowski, F.; Jerzykiewicz, M.; Golonka, I.; Drozd, J.; Bylinska, E.; Chen, Y.; Seaward, M. R. D. Quantitative EPR Study on Free Radicals in the Natural Polyphenols Interacting with Metal Ions and Other Environmental Pollutants. *Spectrochem. Acta, Part A* **2002**, *58*, 1293.
- (45) Paul, A.; Stösser, T. R.; Zehl, A.; Zwirnmann, E.; Vogt, R. D.; Steinberg, C. E. W. Nature and Abundance of Organic Radicals in Natural Organic Matter: Effect of PH and Irradiation. *Environ. Sci. Technol.* **2006**, *40* (19), 5897–5903.
- (46) Li, Y.; Zou, Y. Conjugated Polymer Photovoltaic Materials with Broad Absorption Band and High Charge Carrier Mobility. *Adv. Mater.* **2008**, 20 (15), 2952–2958.
- (47) Lee, J.; Head-Gordon, M. Distinguishing Artificial and Essential Symmetry Breaking in a Single Determinant: Approach and Application to the C60, C36, and C20 Fullerenes. *Phys. Chem. Chem. Phys.* **2019**, 21 (9), 4763–4778.
- (48) Sun, Z.; Zeng, Z.; Wu, J. Zethrenes, Extended p-Quinodimethanes, and Periacenes with a Singlet Biradical Ground State. *Acc. Chem. Res.* **2014**, 47 (8), 2582–2591.
- (49) Goto, A.; Scaiano, J. C.; Maretti, L. Photolysis of an Alkoxyamine Using Intramolecular Energy Transfer from a Quinoline Antenna Towards Photo-Induced Living Radical Polymerization. *Photochemical and Photobiological Sciences* **2007**, *6* (8), 833–835.

- (50) Thomas, R. N. Acid Catalyzed Fullerenation of Carbazole Polymer. J. Polym. Sci., Part A: Polym. Chem. 1994, 32, 2727.
- (51) Gidron, O.; Varsano, N.; Shimon, L. J. W.; Leitus, G.; Bendikov, M. Study of a Bifuran vs. Bithiophene Unit for the Rational Design of π -Conjugated Systems. What Have We Learned? *Chem. Commun.* **2013**, 49 (56), 6256–6258.
- (52) Di Motta, S.; Negri, F.; Fazzi, D.; Castiglioni, C.; Canesi, E. V. Biradicaloid and Polyenic Character of Quinoidal Oligothiophenes Revealed by the Presence of a Low-Lying Double-Exciton State. *J. Phys. Chem. Lett.* **2010**, *1* (23), 3334–3339.
- (53) Shi, X.; Quintero, E.; Lee, S.; Jing, L.; Herng, T. S.; Zheng, B.; Huang, K. W.; López Navarrete, J. T.; Ding, J.; Kim, D.; Casado, J.; Chi, C. Benzo-Thia-Fused [: N] Thienoacenequinodimethanes with Small to Moderate Diradical Characters: The Role of pro-Aromaticity versus Anti-Aromaticity. *Chem. Sci.* **2016**, *7* (5), 3036–3046.
- (54) Ni, Y.; Lee, S.; Son, M.; Aratani, N.; Ishida, M.; Samanta, A.; Yamada, H.; Chang, Y.-T.; Furuta, H.; Kim, D.; Wu, J. A Diradical Approach towards BODIPY-Based Dyes with Intense Near-Infrared Absorption around $\lambda = 1100$ Nm. *Angew. Chem.* **2016**, *128* (8), 2865–2869.
- (55) Hackley, P. C.; Jubb, A. M.; Burruss, R. C.; Beaven, A. E. Fluorescence Spectroscopy of Ancient Sedimentary Organic Matter via Confocal Laser Scanning Microscopy (CLSM). *Int. J. Coal Geol* **2020**, 223, No. 103445.
- (56) Sander, W. Carbonyl Oxides: Zwitterions or Diradicals? *Angew. Chem.* **1990**, 29, 344.
- (57) Kamada, K.; Ohta, K.; Shimizu, A.; Kubo, T.; Kishi, R.; Takahashi, H.; Botek, E.; Champagne, B.; Nakano, M. Singlet Diradical Character from Experiment. *J. Phys. Chem. Lett.* **2010**, *1* (6), 937–940.
- (58) Su, Y.; Wang, X.; Wang, L.; Zhang, Z.; Wang, X.; Song, Y.; Power, P. P. Thermally Controlling the Singlet-Triplet Energy Gap of a Diradical in the Solid State. *Chem. Sci.* **2016**, *7* (10), 6514–6518.
- (59) Chen, H.; Maryasov, A. G.; Rogozhnikova, O. Y.; Trukhin, D. V.; Tormyshev, V. M.; Bowman, M. K. Electron Spin Dynamics and Spin-Lattice Relaxation of Trityl Radicals in Frozen Solutions. *Phys. Chem. Chem. Phys.* **2016**, *18*, 24954.
- (60) Feng, Z.; Chong, Y.; Tang, S.; Fang, Y.; Zhao, Y.; Jiang, J.; Wang, X. A Stable Triplet Diradical Emitter. *Chem. Sci.* **2021**, *12* (45), 15151–15156.
- (61) Wang, Z.; Yadav, P.; Abe, M. Long-Lived Localised Singlet Diradicaloids with Carbon-Carbon π -Single Bonding (C- π -C). Chem. Commun. 2021, 57 (86), 11301–11309.
- (62) NIST. Atomic Reference Data for Electronic Structure Calculations, Atomic Total energies and Eigenvalues. https://www.nist.gov/pml/Atomic Reference Data for Electronic Structure Calculations/Atomic reference data electronic 7.
- (63) Theoretical Study of Thieno[3,4-d]Thiepin and Furo[3,4-d] Thiepin as Dienes in the Diels-alder Reaction.
- (64) Stuyver, T.; Danovich, D.; Shaik, S. Captodative Substitution Enhances the Diradical Character of Compounds, Reduces Aromaticity, and Controls Single-Molecule Conductivity Patterns: A Valence Bond Study. J. Phys. Chem. A 2019, 123 (32), 7133–7141.
- (65) Liu, C.-H.; He, Z.; Ruchlin, C.; Che, Y.; Somers, K.; Perepichka, D. F. Thiele's Fluorocarbons: Stable Diradicaloids with Efficient Visible-to-Near-Infrared Fluorescence from a Zwitterionic Excited State. *J. Am. Chem. Soc.* **2023**, *145* (29), 15702–15707.
- (66) Nakano, M.; Yoneda, K.; Kishi, R.; Takahashi, H.; Kubo, T.; Kamada, K.; Ohta, K.; Champagne, B.; Botek, E. One- and Two-Photon Absorptions in Open-Shell Singlet Systems. *AIP Conf. Proc.* **2012**, *1504*, 136–142.